

Primary drainage of NAPL governed by time-dependent interfacial properties

DAVID M. TUCK

NAPLogic, Inc., P.O. Box 72, Princeton, NJ 08542-0072, USA
Email: dtuck@naplogic.com

Abstract—Primary drainage involving a non-aqueous phase liquid (NAPL) invading a water-saturated, initially water-wet porous medium is a process having important practical interest. It occurs during release of organic liquid contaminants such as gasoline, solvents, or other organic wastes. It also occurs during primary migration of oil following its generation in a source zone. Standard conceptual and numerical pore-scale models of this process do not incorporate time in any explicit manner in their representation of the capillary forces that control this process. Time-dependence of interfacial chemistry, however, is a well-known phenomenon, with some of the earliest interfacial chemical work exhibiting its existence, and quantitative evaluation becoming established in the late 1930's. Time-dependence of interfacial properties is manifested during primary drainage through the sequential processes of interface dilation and compression as a fluid-fluid interface advances through a porous medium. This sequence is illustrated and described schematically to demonstrate its importance in the drainage process.

Log-linear interfacial chemical kinetics of a known system was incorporated into a small pore-scale model to assess its influence on primary drainage. NAPL saturation was a function of time as well as applied capillary pressure. NAPL migration rate became a log-linear function of applied capillary pressure, and the maximum NAPL saturation exhibited a minimum at the entry pressure for pure bulk NAPL without any interfacially active components. This arises from competition between applied capillary pressure and the interfacial kinetics for control over the timing of when and whether NAPL penetrates a given pore or not. The interfacial chemical kinetics dominate at lower applied capillary pressure. More time becomes available for the interfacial chemical kinetics to lower interfacial tension sufficiently to enter pores that would otherwise be by-passed as the applied capillary pressure decreases. These results stand in marked contrast with the "standard" equilibrium view of the capillary pressure-saturation relationship. Comparison of model results, assuming standard Tempe cell dimensions, indicates initial penetration of a medium occurs at lower capillary pressure and final saturation is higher when time-dependent interfacial chemistry is incorporated.

1. INTRODUCTION

Subsurface non-aqueous phase liquid contamination, both light (LNAPL) and dense (DNAPL), poses a major environmental problem for many commercial and industrial sites. For the purposes of this paper, NAPL, LNAPL, and DNAPL are interchangeable; the behavior will be comparable with respect to the interfacial chemistry. Understanding DNAPL behavior in porous media is important for designing effective strategies for locating subsurface DNAPL and for designing effective remediation systems. The displacement of water by a non-aqueous phase liquid (NAPL) is called primary drainage. It is also important for petroleum migration from a source area. Two important interfacial properties play major roles in subsurface NAPL movement during primary drainage: the surface or interfacial tension between fluids and the contact angle between the fluid-fluid interface and the mineral-grain solid surfaces. "Surface tension" is generally applied to gas-liquid systems, while "interfacial tension" is applied to liquid-liquid systems.

Interfacial properties are generally treated as static by assuming equilibrium values when modeling multi-

phase behavior in porous media, either explicitly in pore-scale models or implicitly in continuum models. This assumption is accurate for three cases: 1) single component NAPLs, 2) systems where the magnitude of the kinetic changes are small with respect to the equilibrium values, or 3) systems where the interfacial chemical kinetics are rapid with respect to the process under consideration. Interfacial chemical kinetics involves the rates of interfacial reactions, such as partitioning of surface active substances into a fluid-fluid interface. Assuming equilibrium, however, is not necessarily accurate for the process of primary drainage (i.e., initial penetration of a water-wet porous medium by a NAPL). The first objective of this paper is to briefly review literature on time-dependent interfacial chemistry to show it is not a new or unknown phenomenon. The second objective is to illustrate why equilibrium is not necessarily a valid *a priori* assumption with respect to primary drainage, and how time-dependent interfacial effects are manifested during primary drainage. The final objective is to show the effects of incorporating time-dependent interfacial chemistry in a small pore-scale model.

1.1. Time-Dependence in Interfacial Chemistry

Early indications that interfacial chemical equilibrium is not established instantaneously are over a hundred years old. Tate (1864) showed that interfacial tension of solutions measured using the drop volume method depends on the rate of formation of the drop. The faster a drop is formed (i.e., the younger its average surface age), the higher is the measured interfacial tension. Dupré (1869) studied the surface tensions of aqueous soap solutions, noting that they decreased as the surface aged. Lord Rayleigh (1879) developed the pulsating jet method for measuring surface tension, and later (Rayleigh, 1890) showed it could be used to resolve surface tension changes over short time-scales (on the order of seconds). Rayleigh also concluded that surface tension of sodium oleate solutions decreased with increasing age of the surface. Bohr (1909) further developed and refined the vibrating or oscillating jet method, facilitating its application by later workers (Rideal and Sutherland, 1952; Addison and Litherland, 1953; Thomas and Potter, 1975; Zhang and Zhao, 1989). Several research groups used other methods to show that surface tension of aqueous soap solutions varied with time (Bigelow and Washburn, 1928; Tartar et al., 1940). Andreas et al. (1938) extended and further developed the pendant drop technique for measuring surface and interfacial tensions. Ward and Tordai (1944) showed that the interfacial tension of solutions is, in general, time-dependent. Later, Ward and Tordai (1946) were the first to explicitly apply a diffusion model to fit kinetic data for interfacial tension. Several authors have since measured time-dependent surface or interfacial tension covering many orders of magnitude in time scales. Time-scales of interfacial or surface tension kinetics range from milliseconds (Thomas and Potter, 1975; Zhang and Zhao, 1989) to seconds and minutes (Lucassen and Giles, 1975; Tuck and Rulison, 1999a), to minutes and hours (Pan et al., 1998), to hours, days, and longer (Tartar et al., 1940; Schroth et al., 1995; Tuck and Rulison, unpublished data; Tuck and Rulison, 1999a).

Time-dependence in interfacial chemistry is thus a well-known phenomenon. This time-dependence can occur over a very large range of time scales, depending on the system under consideration. It is therefore not necessarily appropriate to *assume* equilibrium values for interfacial tension and contact angle. Tuck and co-workers (Tuck et al., 1998) have shown that the *effective* value of interfacial tension between water and a dyed-DNAPL may vary significantly during primary drainage when interfacial chemical kinetics is considered. They showed that the faster a penetrating front of a complex NAPL (exhibiting

time-dependent surface chemistry) penetrates a porous medium, the younger will be the average interface age, and therefore the higher will be *effective* interfacial tension. Whether or not equilibrium values will accurately reflect their *effective* values during primary drainage of a complex NAPL in an initially water-wet porous medium depends on the relative time scales of the drainage process and the interfacial chemical kinetics. It is inappropriate to assume equilibrium values measured for pure phases when modeling the behavior of complex phases. Examples of these situations include DNAPLs stained with an azo dye (Tuck and Rulison, 1999b) or field NAPLs such as gasoline or spent solvents (Powers and Tamblin, 1995; Tuck et al., 1998).

The mechanism through which time-dependent interfacial properties are manifested during primary drainage is illustrated in a later section. The potential influence of interfacial chemical kinetics on primary drainage is demonstrated in the subsequent section through the development and implementation of a pore-scale model in which time-dependent interfacial tension is incorporated.

1.2. Theory

1.2.1. Surface chemistry and pore-scale interface movement

Interfacial chemistry is important in multiphase flow in porous media because of its role in capillary forces. Capillary forces determine which pores will be penetrated by an infiltrating NAPL during primary drainage. This role is expressed through the Young-Laplace equation (Dullien, 1992):

$$P_c = P_n - P_w = \gamma_{nw} \cos \theta \left(\frac{1}{r_1} + \frac{1}{r_2} \right) \quad (1)$$

where P_c is the capillary pressure (dynes/cm² or N/m²), which is defined as the difference between the non-wetting phase pressure P_n and the wetting phase pressure P_w , γ_{nw} is the interfacial tension between the nonwetting (*n*) and wetting (*w*) fluid phases (dynes/cm or mN/m), θ is the contact angle between the fluid-fluid interface and the solid or mineral surface (degrees or radians), and r_1 and r_2 are the principal radii of curvature of the fluid-fluid interface (cm or m). The two radii of curvature are equal if the capillary geometry is cylindrical, in which case the Young-Laplace equation simplifies to:

$$P_c = P_n - P_w = 2 \gamma \cos \theta \left(\frac{1}{r} \right) \quad (2)$$

Typically, pore-scale models of porous media assume circular cross-sectional geometry for the structure of pores and pore-throats (Celia et al.,

1995). The interfacial tension (γ) and contact angle (θ) are represented as single-valued, i.e., equilibrium, parameters in most pore-scale models, or contact angle hysteresis is incorporated by specifying advancing and retreating contact angles (Giordano and Slattery, 1983a; Dullien, 1992). Equation 2 (or appropriate modifications) is used to determine interface stability and thus whether an immiscible fluid phase (gas or NAPL) penetrates a given pore during primary drainage. A fluid-fluid interface may be "trapped" in a given pore throat until conditions change to make it unstable.

A fluid-fluid interface is unstable once it passes the neck of a pore throat (Haines, 1930; Miller and Miller, 1956; Melrose, 1965; Dullien, 1992). The interface advances extremely rapidly through the pore-body into the next pore throats where it reestablishes new stable positions. This rapid interface "jump" is called a Haines jump, named after the person who first described it (Haines, 1930). Interface migration through a porous medium occurs through a sequence of relatively stable locations in pore throats linked by a series of Haines jumps. The applied capillary pressure controls stable interface locations in a model porous medium (and within any given pore if the pore-throat geometry is allowed to change with axial distance through the pore-throat). This is because most models treat the interfacial chemistry as static via equilibrium assumptions for γ and θ . The interface locations within a pore-throat will change, however, if interfacial chemistry is not at equilibrium and capillary pressure is not sufficiently high to overcome the initial capillary forces.

1.2.2. Interfacial chemical kinetics

Equilibrium values of interfacial tension or contact angle are determined by partitioning or adsorption equilibria of interfacially active (surface active) components at the interfaces whenever any of the phases contain such components. This is expressed quantitatively via the Gibbs equation (Gibbs, 1948; Adamson, 1990). The Gibbs equation for a three-component system at constant temperature is (Adamson, 1990):

$$d\gamma = -\Gamma_1^\sigma d\mu_1 - \Gamma_2^\sigma d\mu_2 - \Gamma_3^\sigma d\mu_3 \quad (3)$$

where Γ_i^σ is the surface excess of component i , μ_i is chemical potential of component i , and the superscript σ designates that the parameter is evaluated at the surface between the fluid phases. In this paper, components 1 and 2 are the respective bulk fluids. Component 3 is assumed to be interfacially active; it may be either predominantly present in the aqueous phase (water soluble) or predominantly present in the

NAPL (oil soluble). Positive surface excess means that a greater amount of component i is accumulated in the surface than is present in a volume of bulk solution containing the same amount of solvent. A reduction in interfacial tension occurs in such cases. The first two terms of Eqn. 3 can be eliminated if we assume that a Gibbs surface equation (Gibbs, 1948; Adamson, 1990) can be defined, i.e., if we define a surface such that $\Gamma_1^\sigma = \Gamma_2^\sigma = 0$.

Equation 3 is an equilibrium equation. The surface excess of component 3, Γ_3^σ (and therefore the interfacial tension between the liquid phases) changes with time if surface equilibrium has not been attained. Isothermal perturbation of a surface equilibrium can be brought about in five ways: 1) addition of pure component 1 to the bulk liquid 1 phase, 2) addition of pure component 2 to the bulk liquid 2 phase, 3) addition of component 3 to either of the liquid phases, 4) compression of the interfacial area, or 5) dilation of the interfacial area. The first three ways change the chemical potentials, μ_i , the fourth way increases the surface excess, and the fifth decreases the surface excess.

Time becomes an important variable for interfacial tension when an interface is expanding or being compressed more rapidly than interfacially-active components in either phase can partition into or out of the interface. Time-dependence is a function of the specific system and varies over several orders of magnitude of time-scale, as noted in the introduction. Time-dependence of interfacial tension during a dilation process is also known as *dynamic surface* or *interfacial tension* (Lucassen and Giles 1975) and as *surface dilational viscosity* (Giordano and Slattery, 1983a, b, 1987). The latter term arises by analogy that interfacial tension resists interface dilation as viscosity resists fluid flow. Interfacial chemical kinetics may become important for any given dynamic process involving compression or dilation of fluid-fluid interfaces. Imbibition, the immiscible displacement of a non-wetting fluid by a wetting fluid in a porous medium, and drainage, the immiscible displacement of a wetting fluid by a non-wetting fluid in a porous medium, are two such processes.

1.2.3. "Haines" jumps and interface dilation

Crawford and Hoover (1966) examined the movement of air-water interfaces through small diameter glass and Teflon tubes (ID \cong 1 mm) filled with various sized water-wetted or non-wetted beads. They simultaneously monitored injection pressure (in cm of water) and injection volume, which was done in discrete volumetric increments, $\Delta V = 1.7 \times 10^{-4}$ cm³. Their pressure plots show distinct discontinuities, which

Crawford and Hoover associated with rapid movements of the air-water interfaces as they advanced from pore-to-pore, i.e., the pressure discontinuities correspond to Haines jumps. The discontinuities occurred in less than 0.5 seconds (the approximate limit of time resolution in their measurements) in pores with volumes ranging in size from approximately 0.5 to $14 \times 10^{-5} \text{ cm}^3$. These pore dimensions are roughly the scale of medium to very coarse sand. Thus, 0.5 seconds is a measure of the upper limit for the time required for an air-water interface to advance through a single pore-body during a Haines jump in their media. The "creeping" stages occurred over time-spans ranging between approximately 20 and 185 seconds. These results indicate that air-water interfaces spent at least 40 times longer in pore-throats than in "jumping" to the next pore throat, and that ratio may exceed 400. Thus, the assumption that interfaces spend negligible time moving through pore bodies is a reasonable first approximation (Tuck et al., 1998).

Heller (1968) took 16-mm movies (64 frames per second) of drainage experiments of 1,1,1-trichloroethane from two unconsolidated packs of 80-mesh and 140-mesh fluorite grains. Exposure time was half of the 15.6-millisecond frame-repetition-time. He documented Haines jumps covering a few pores (~1 to 10 by visual estimation) and several covering several tens of pores occurring over the time interval between exposures. Therefore these Haines jumps took place in no more than 23.4 milliseconds. Haines jumps covering several tens of pores imply that relatively small regions in the porous medium have slightly larger pore-throat sizes than the surrounding porous regions.

1.2.4. Interfacial viscosity

Boussinesq (1913), in his analysis of free-boundary flows, identified two coefficients of interfacial viscosity, interfacial shear viscosity (ϵ) and interfacial dilational viscosity (κ). These interfacial viscosity coefficients are incorporated into the standard Newtonian model for fluid interfaces (Scriven, 1960; Slattery, 1964). Interfacial shear viscosity is the two-dimensional equivalent of the ordinary fluid shear viscosity; it is the force required to produce relative motion between adjacent line elements in a surface (Adamson, 1990). Surface or interfacial dilational viscosity is defined by the following equation (Adamson, 1990):

$$\frac{1}{\kappa} = \frac{1}{\Delta\gamma} \frac{1}{A} \frac{dA}{dt} \quad (4)$$

where γ is the surface or interfacial tension, A is the interfacial area, and t is time. He notes that the equi-

librium quantity corresponding to κ is the modulus of surface elasticity, E , given by:

$$E = \frac{d\gamma}{d \ln A} \quad (5)$$

He further states that "... κ and E are probably the most important rheological properties of interfaces and films" (Adamson, 1990, p. 127). Of the two coefficients of surface viscosity, interfacial dilational viscosity is generally more important for two reasons: first, κ is generally on the order of 100 times greater than ϵ ; and second, interfaces are more often subject to dilation strains than shear strains (Adamson, 1990).

1.2.5. Interfacial compression and dilation in porous media

Fluid-fluid interfaces continually go through compression and dilation during drainage or imbibition. Drainage in a porous medium is illustrated in Fig. 1, which is a qualitative time sequence showing the advance of a multicomponent fluid containing a surface active component ($i = 3$) through an idealized pore. The porous medium is visualized as a vertical slice through uniform, spherical grains in a cubic packing (Graton and Fraser, 1935). The appropriate equilibrium interfacial tension equation is Eqn. 3, assuming isothermal conditions and a Gibbs' surface. The surface excess, Γ_3^σ , is illustrated schematically by a surfactant molecule partitioned across the fluid-fluid interface; each surfactant molecule shown in the interface represents a schematic surface excess of one (1). The initial stage, shown in Fig. 1a, is taken to be a "fresh" interface, just established in the top pore-throat, and the schematic surface excess equals 2. The hydrostatic fluid pressure difference is assumed to remain constant.

Component 3 diffuses to and partitions into the interface as the interface ages. The surface excess increases and interfacial tension decreases. The stable position of the interface changes as a result, and the interface begins to creep down into the pore throat. The interfacial area is compressed simultaneously with the creeping interface advance. Both processes, adsorption of component 3 and interface compression, act to increase the surface excess, Γ_3^σ , and thus decrease interfacial tension according to Eqn. 3. Schematic surface excess in Fig. 1b is designated as 4^+ , with the superscript "+" indicating the surface compression portion of the increased surface excess. These processes continue until the interface reaches the neck of the pore throat, where, in Fig. 1c, the schematic surface excess is 6^{++} .

A Haines jump results in extremely rapid dilation of the interface as illustrated in the sequence pro-

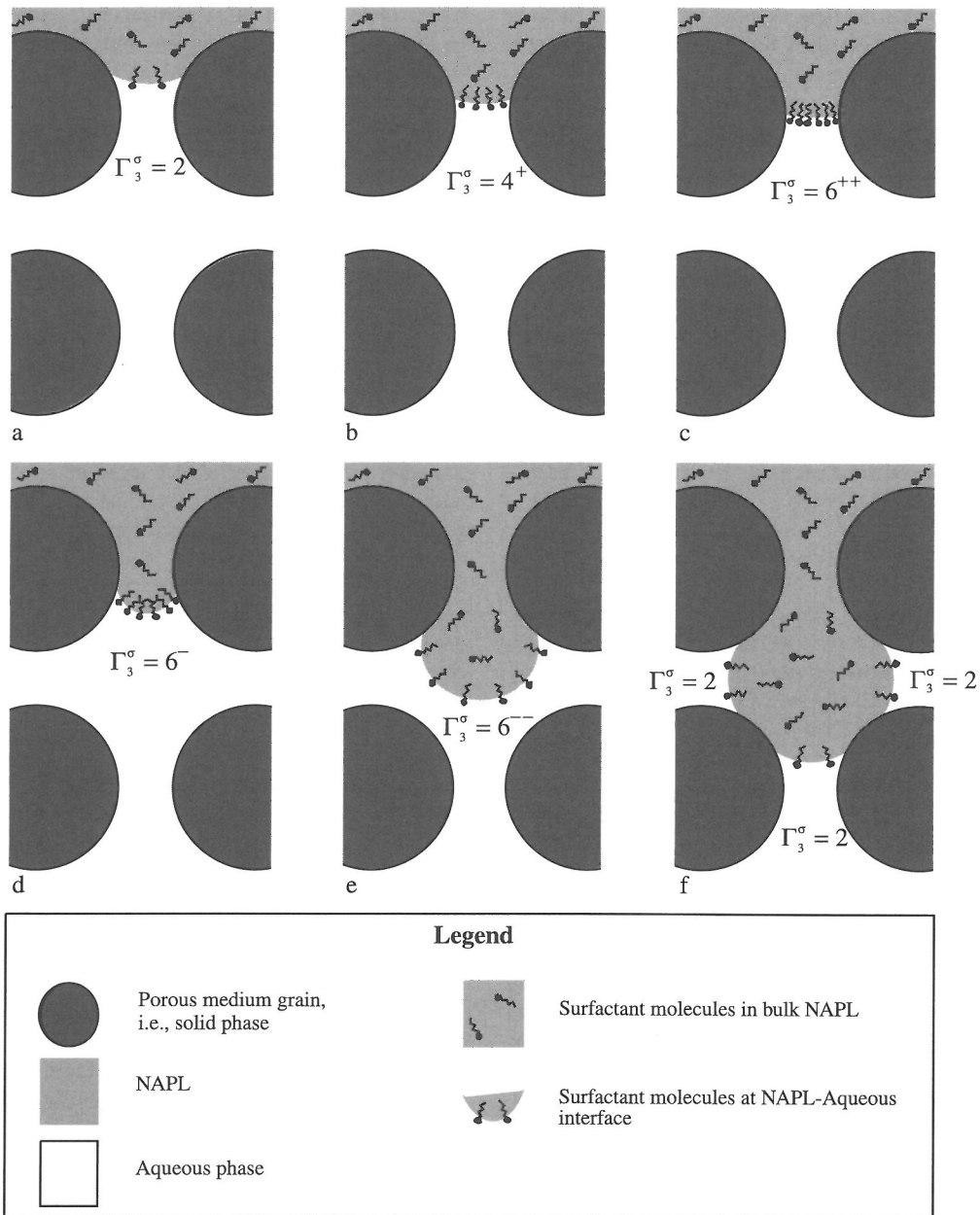


Fig. 1. Schematic illustration of the mechanism by which dynamic interfacial tension effects are manifested during primary drainage in a porous medium. The schematic values of the surface excess, Γ_3^σ , are displayed. See text for discussion.

ceeding from Figs. 1c-f. Following the method above, the schematic surface excess in Fig. 1d is 6^- , and by Fig. 1e it is 6^{--} , with the superscript “-” indicating decreased surface excess due to surface dilation. The surface excess continues to decrease, purely by dilation, and, by the time the “jumping” interface

encounters the three new pore throats and establishes three new semi-stable interfaces, it has decreased, in this idealized medium, back to 2, where the sequence started. This schematic sequence illustrates how interfacial chemical kinetics becomes important during multiphase flow in porous media. The sequence

assumes that the time required for a Haines jump is significantly less than the time required to attain interfacial equilibrium.

1.2.6. Early modeling work

Giordano and Slattery (1983a, b) extended the qualitative theory proposed by Slattery (1974, 1979) in their model of immiscible displacement of a NAPL blob in a capillary of constant radius incorporating the influence of interfacial viscosity. One of their major explicit assumptions was that the dimensionless interfacial viscosity, $N_{\kappa+\varepsilon}$, is much greater than unity. $N_{\kappa+\varepsilon}$ is the ratio of the sum of the interfacial shear ε and dilational viscosity κ to the bulk fluid shear viscosity-capillary radius product ($\mu_2 R$); here the subscript 2 indicates the bulk viscosity of the discontinuous fluid phase:

$$N_{\kappa+\varepsilon} = \frac{\kappa + \varepsilon}{\mu_2 R} \quad (6)$$

Giordano and Slattery (1983a, b) concluded that interfacial viscosity could have a significant effect on tertiary oil recovery, and that the interfacial dilational viscosity was of greater importance than interfacial shear viscosity. They also showed that rate of displacement is a function of interfacial viscosity.

In a later paper, Giordano and Slattery (1987) modeled immiscible displacement of a NAPL blob in a capillary whose radius varies in sinusoidal fashion with axial position. Again, they found that interfacial viscosity played a major role in determining the average rate of displacement. Quasi-stable interfaces are established as an interface begins into the narrow portion of the sinusoidal capillary. They creep slowly toward the neck of the pore throat. Beyond this point the interfaces become unstable, and "jump" to the next pore throat where they begin the slow "creeping" stage anew. Their 1983 and 1987 models, however, did not consider the effects involved with the multiply-connected pores of a 2-D or 3-D porous medium network.

The rate at which a non-wetting, immiscible phase penetrates a porous medium is strongly controlled by the amount of time the interfaces spend "creeping" down into the pore throats until they reach their unstable limit at the pore necks (Miller and Miller, 1956; Melrose, 1965; Giordano and Slattery, 1983b, 1987). In the traditional view, this is purely a function of the applied fluid pressure difference, i.e., capillary pressure. Applied capillary pressure is not the only control, however, for complex fluids. The time-dependence of interfacial chemistry can play a major role in such systems. As noted above, Giordano and Slattery (1983a) showed that displacement rate of

NAPL blobs trapped in cylindrical and sinusoidal capillaries is a function of dimensionless interfacial viscosity. Also, Tuck et al. (1998) showed that different *effective interfacial tension* values are likely to apply when the physical capillary pressure exceeds the entry pressure for the medium. A small pore-scale model is developed in the next section to examine the effects of time-dependent interfacial tension (i.e., *dynamic interfacial tension* or *interfacial dilational viscosity*) on primary drainage in porous media.

2. PORE-SCALE MODEL

2.1. Model Domain

A small, two-dimensional pore-scale model was formulated consisting of a 7x7 array of spherical pore bodies connected by cylindrical pore throats arranged in a square lattice (see Fig. 2). The pore throats were assumed to be of infinitesimal length, and hence did not contribute to the pore volume. Two populations of pore body and pore throat sizes were designed to mimic fine-to-medium sand, based on empirical results of Pirkle et al. (1997a). Figure 3 is a graphical presentation of the data contained in Tables 1 and 2. Five evenly-spaced pore-body and pore-throat sizes were assigned to each population. The populations shared one overlapping category of pore-body and pore-throat size. The central nine pores of the medium were assigned the smaller pore-body and pore-throat size-categories. Pore-body and pore-throat sizes were assigned randomly by my assistant (my, at that time, three-year old daughter, Gaia) by drawing cards from a shuffled deck consisting of aces through fives. The horizontal boundaries of the medium are no-flow boundaries. The upper boundary of the medium is a constant non-wetting-phase pressure boundary. The lower boundary is a constant wetting-phase pressure boundary. For the sake of convenience, the term "capillary pressure" will be used interchangeably for the "boundary fluid pressure difference". In reality, "capillary pressure" means the fluid-pressure difference existing across a specific NAPL-water interface. This will vary throughout the model, with values below the applied fluid-reservoir pressure difference. The pore throats at the boundaries fall in the coarser pore-throat size population. Tables 1 and 2 contain the pore body and pore throat size specifications, respectively, corresponding to the different size categories. This pore-scale model can be conceived, in physical terms, as a two-dimensional slice through a granular medium containing a random heterogeneity, either due to packing variation of uniform grains (Graton and Fraser, 1935) or variation in

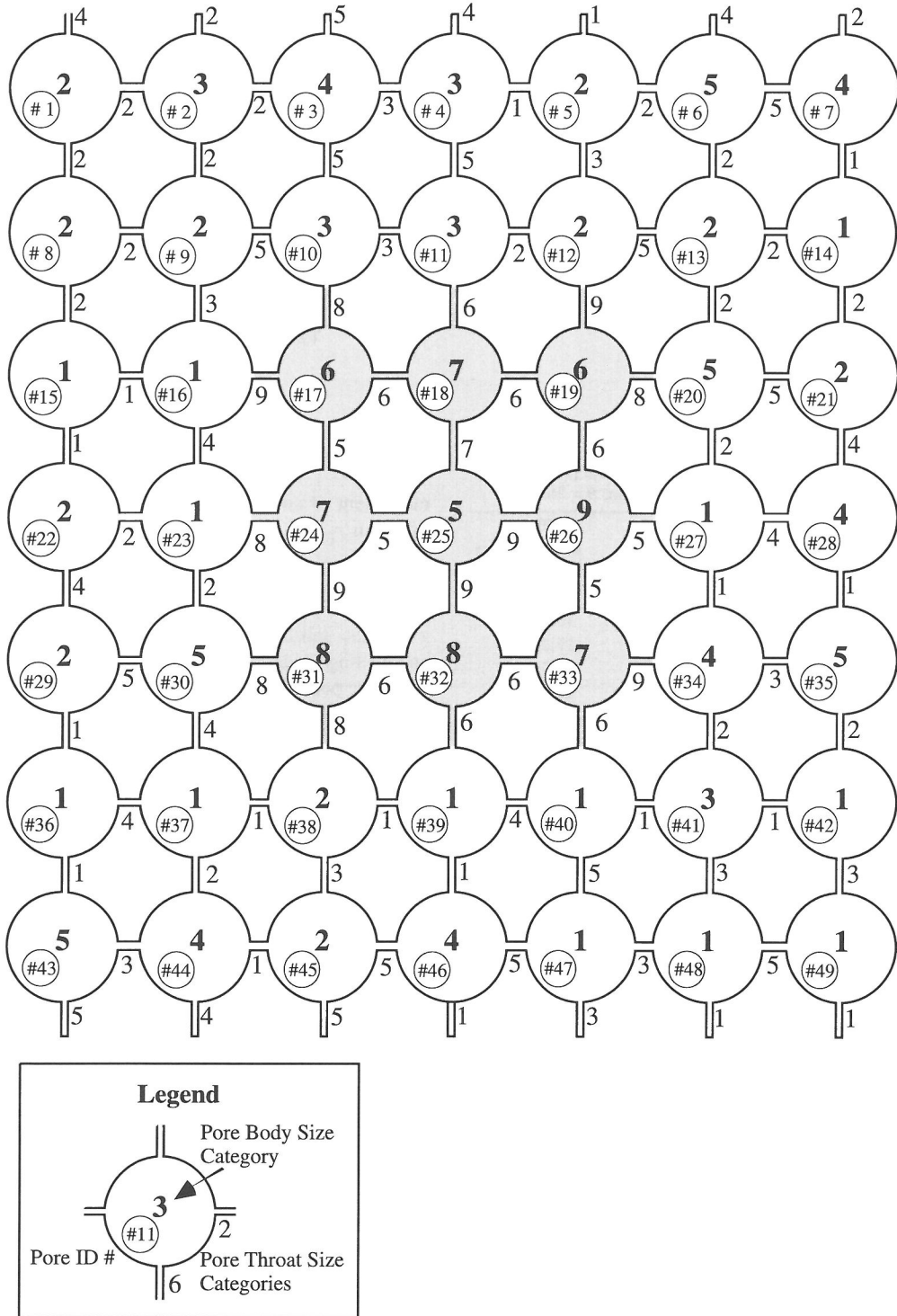


Fig. 2. Time-dependent interfacial chemistry effects were assessed in this 7x7 node pore-scale model. The center nine pores (nodes) and associated pore-throats were assigned to the smaller size range. Pore-body and pore-throat sizes are given in Table 1.

Table 1. Pore-body and pore-throat size categories and pore volumes.

Pore Category Number	Pore Radius (cm ³ , x10 ⁻²)	Volume per Pore (cm ³ , x10 ⁻⁴)	Number of Pores in Category	Total Volume for Size Category (cm ³ , x10 ⁻³)
1	5.4	6.5958	13	8.58
2	5.2	5.8898	11	6.48
3	5.0	5.2350	5	2.62
4	4.8	4.6325	6	2.78
5	4.6	4.0772	6	2.45
6	4.4	3.5682	2	0.713
7	4.2	3.1034	3	0.931
8	4.0	2.6808	2	0.536
9	3.8	2.2985	1	0.230
Total Pore Volume				25.3

Table 2. Pore throat size categories and pore entry pressures for PCE ($\gamma = 48.6$ mN/m, $\theta = 26.5^\circ$).

Pore Throat Category	Pore Throat Radius (cm)	Capillary Entry Pressure (mbar)
1	5.4×10^{-3}	16.04
2	5.2×10^{-3}	16.62
3	5.0×10^{-3}	17.26
4	4.8×10^{-3}	18.01
5	4.6×10^{-3}	18.79
6	4.4×10^{-3}	19.64
7	4.2×10^{-3}	20.58
8	4.0×10^{-3}	21.61
9	3.8×10^{-3}	22.74

grain size (Morrow, 1971). Alternatively, it could be conceived as a model of a rough walled fracture with the central region being of smaller average aperture.

The drainage experiment results reported by Heller (1968) provide support for including small-scale heterogeneous regions within a pore-scale model. As mentioned above, Haines jumps covering several tens of pores imply relatively small regions within the medium that have slightly larger, effective pore-throat radii. The qualifying term "effective" distinguishes the irregular geometry of real porous media from the idealized representation of cylindrical and spherical geometry used here and in most pore-scale models.

2.2. Incorporating Time-Dependent Interfacial Chemistry

The Young-Laplace equation modified for circular cross-sectional elements (Eqn. 2) governs the capillary behavior. Thus, the standard criterion for

movement of an interface past a given pore throat of radius r_{ij} is:

$$P_c = P_n - P_w > \frac{2\gamma \cos \theta}{r_{ij}} \quad (7)$$

where the subscripts n and w indicate non-wetting and wetting fluids, respectively, and i and j designate a specific pore-throat. This criterion holds for single-valued interfacial tension and contact angles. Trapping of wetting fluid by isolation from continuous wetting fluid was allowed in the model. Wetting fluid becomes trapped in finer pore-body/pore-throat domains as a NAPL penetrates the coarser domains surrounding them. Ferrand and Celia (1992) have shown this to be an important process in heterogeneous porous media. This model was designed to capture this effect on a smaller scale.

When time-dependence is incorporated into the interfacial parameters, the criterion for interface movement through a pore can be specified as:

$$P_c = P_n - P_w > \frac{2\gamma(t) \cos \theta(t)}{r_{ij}} \quad (8)$$

where the interfacial tension, $\gamma(t)$, and contact angles, $\theta(t)$, are each expressed as functions of time.

2.2.1. Interfacial chemical kinetics

Tuck and co-workers (Tuck et al., 1998; Tuck and Rulison, 1999a, b; Tuck and Rulison, unpublished data) have characterized the time-dependence of interfacial tension and contact angle in the Sudan IV-dyed-tetrachloroethylene (PCE)-water-glass system. This system is of interest because several investigators have used this dye in visualization experiments involving PCE or other DNAPLs (Kueper and Frind,

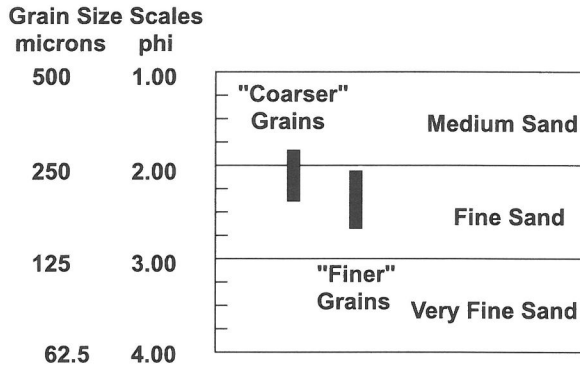


Fig. 3. Comparison of pore-scale model dimensions with approximate dimensions for “equivalent” granular porous media. The two pore-body and pore-throat size populations overlap slightly near the boundary between fine and medium sand.

1991; Poulsen and Kueper, 1992; Brewster et al., 1995; Fortin et al., 1997). Sudan IV belongs to the azo class of dyes (Catino and Farris, 1978). Virtually all visualization studies involving dyed DNAPLs have used this dye or minor variations of it (Tuck, 1999). Tuck and co-workers (Tuck et al. 1998; Tuck and Rulison, 1999a, b) found that both $\gamma(t)$ (expressed in dynes/cm or, equivalently, mN/m) and $\theta(t)$ (expressed in degrees) for a system consisting of 0.5 g/L of Sudan IV in PCE, deionized water, and glass can be described accurately over time spans of hours to days by the following log-linear equations (see Figs. 4 and 5):

$$\gamma(t) = 48.6 - 3.64 \log(t) \quad r^2 = 0.991 \quad (9)$$

$$\theta(t) = 21.4 + 5.96 \log(t) \quad r^2 = 0.933 \quad (10)$$

where t is the age of the interface in seconds. The model applied here simplified Eqn. 8 by assuming an “equilibrium” value for the contact angle (26.5°), i.e., no contact angle time-dependence was assumed. The focus of the modeling work was solely on the effects of time-dependent interfacial tension. The interfacial tension time-dependence was modeled using Eqn. 9, and the critical ages were calculated to satisfy the inequality of Eqn. 8 for each pore-throat size category as a function of applied capillary pressure (see Fig. 6). The log-linear equation results in higher interfacial tension values than for pure PCE for interface ages less than one second. This is unlikely to be physically realized. Hence, any critical age less than one second was taken to indicate the interface was instantly unstable. In such cases, the interface continues into the next pore (or pores) until it encounters a pore-throat of sufficiently small radius to stop it.

2.2.2. Numerical experiments

Three sets of numerical experiments were performed. The first set included two experiments using Eqn. 7, i.e., assuming capillary equilibrium, as the criterion for interface movement, one using 48.6 mN/m for the interfacial tension and the other using 25.3 mN/m (from Eqn. 9 using an interface age of 30 days). These experiments were run assuming the conventional capillary pressure-saturation experimental procedure of incrementing capillary pressure and assuming equilibrium capillary pressure-saturation conditions are achieved following each pressure increment. Capillary pressure was incremented in 0.2 mbar steps for this first set of experiments.

The second set of numerical experiments was run assuming constant fluid reservoir pressure difference P_c throughout an experiment. The constant value of P_c was changed for each experiment in increments of 2 mbar from 2 to 20 mbars for this series of experiments. Near the entry pressure for pure PCE in this medium (approximately 16 mbar), P_c was changed in increments of 1 mbar. The NAPL (PCE) saturation history was then computed for each value of P_c . Viscous flow control of pore-filling times was approximated by assuming that 0.01 seconds was required for all pore-throat and pore-body sizes. Heller’s (1968) experimental documentation of Haines jumps during drainage suggests this time estimate is at least the right order of magnitude. Actual times should vary as a function of the pore-throat radius and length (Blunt and King, 1991). Since infinitesimal length was assumed for each pore-throat, however, a constant value for the fill time is a reasonable first approximation. This only becomes important for pressures above 16 mbar.

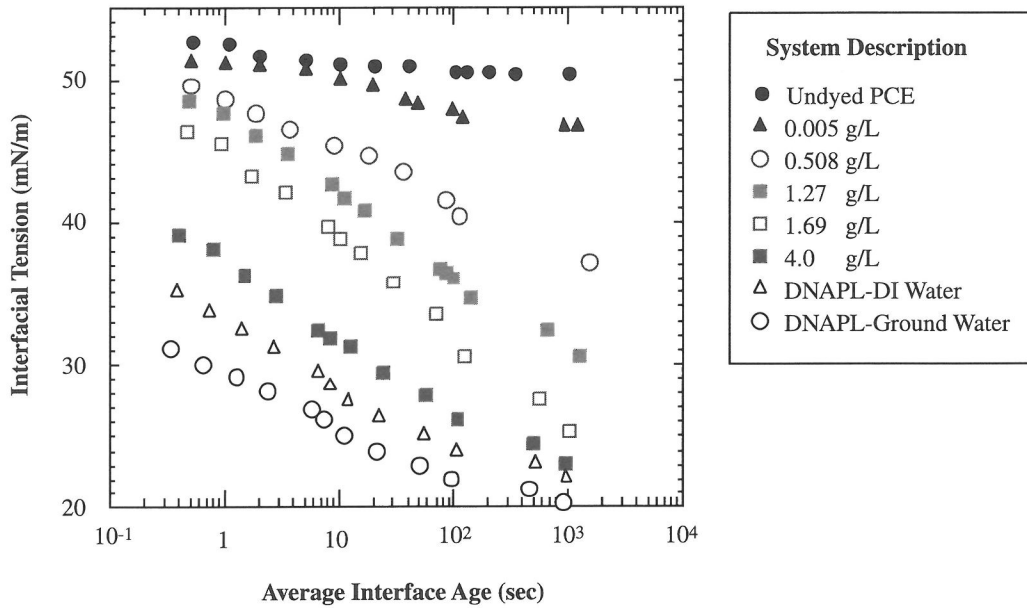


Fig. 4. Time dependence of interfacial tension in the system water-tetrachloroethylene (PCE)-Sudan IV dye. DNAPL-DI water curve is for the surface between a sample of the Savannah River Site A/M Area DNAPL (site DNAPL) and deionized water. DNAPL-Ground Water curve is for the surface between the site DNAPL and an equilibrated sample of the A/M Area ground water.

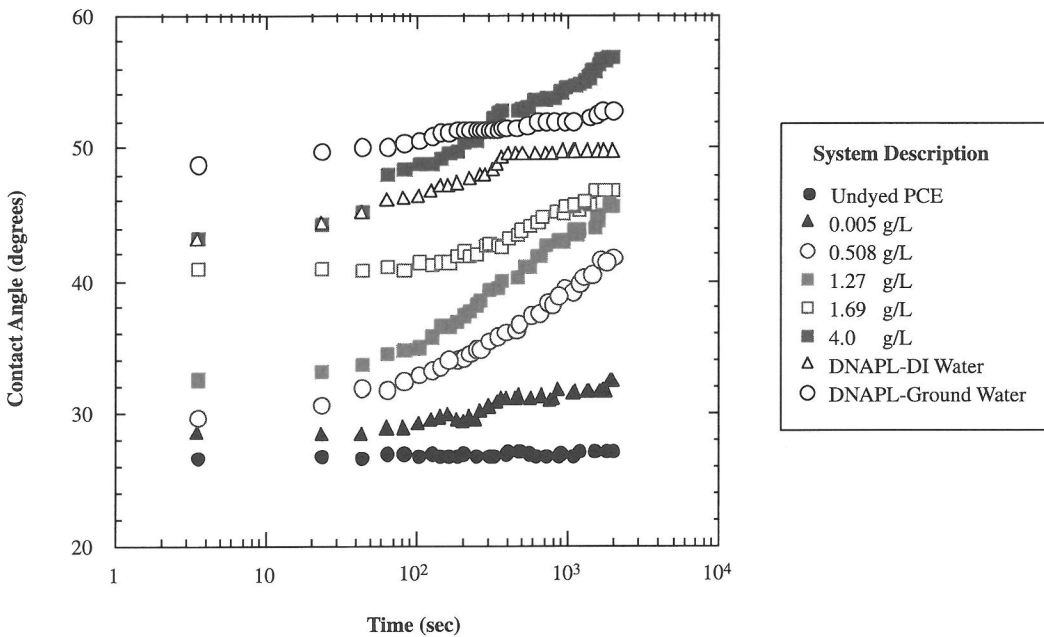


Fig. 5. Time dependence of contact angle in the water-tetrachloroethylene (PCE)-Sudan IV dye-glass system. DNAPL-DI water curve is for the surface between a sample of the Savannah River Site A/M Area DNAPL (site DNAPL) and deionized water. DNAPL-Ground Water curve is for the surface between the site DNAPL and an equilibrated sample of the A/M Area ground water.

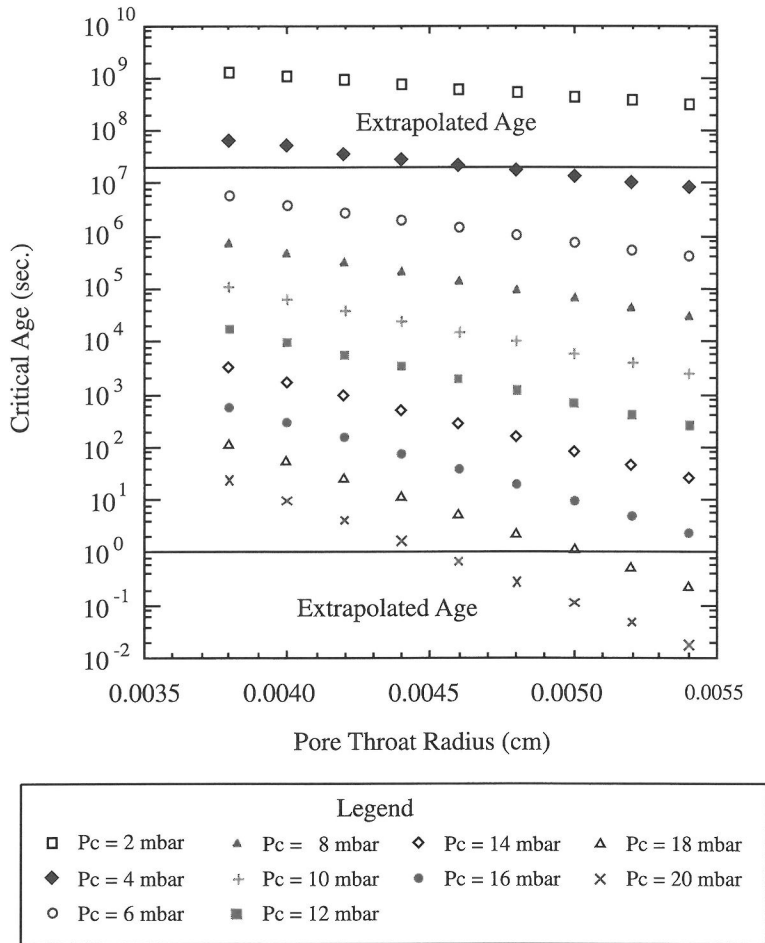


Fig. 6. Critical age for interface instability as a function of applied capillary pressure and pore-throat radius. Critical ages greater than approximately 3×10^6 seconds are extrapolations of the empirical data. Critical ages less than one second indicate conditions in which the pore-throat will not support an interface. Symbols are the calculated results for the model pore-throats listed in Table 2.

The third set of numerical experiments was run as a standard capillary pressure-saturation experiment, but assuming time-dependence of interfacial tension was operating and pressure-step equilibration time (the length of time following each pressure increment) was varied. The pressure was incremented in 2-mbar steps for 2 to 20 mbars, and time-dependent penetration of the medium was recorded for the pressure-step-equilibration time for that experiment. In these last experiments, an interface instantly becomes unstable (i.e., jumps to the next pore) if the age of an interface in a pore-throat was greater than or equal to the critical age for a stable interface at the incremented value of P_c .

3. MODEL RESULTS

3.1. Equilibrium Interfacial Tension

Results from the first set of experiments are shown in Fig. 7. Different values for “equilibrium” interfacial tension were assumed in these experiments. Note that the entry pressure for this medium for undyed PCE is between 16.0 and 16.2 mbars. The maximum NAPL saturation attained in both experiments was 0.8542.

3.2. Time-Dependent Interfacial Tension

Model results for the second set of experiments are presented in Fig. 8. Dynamic interfacial chemistry

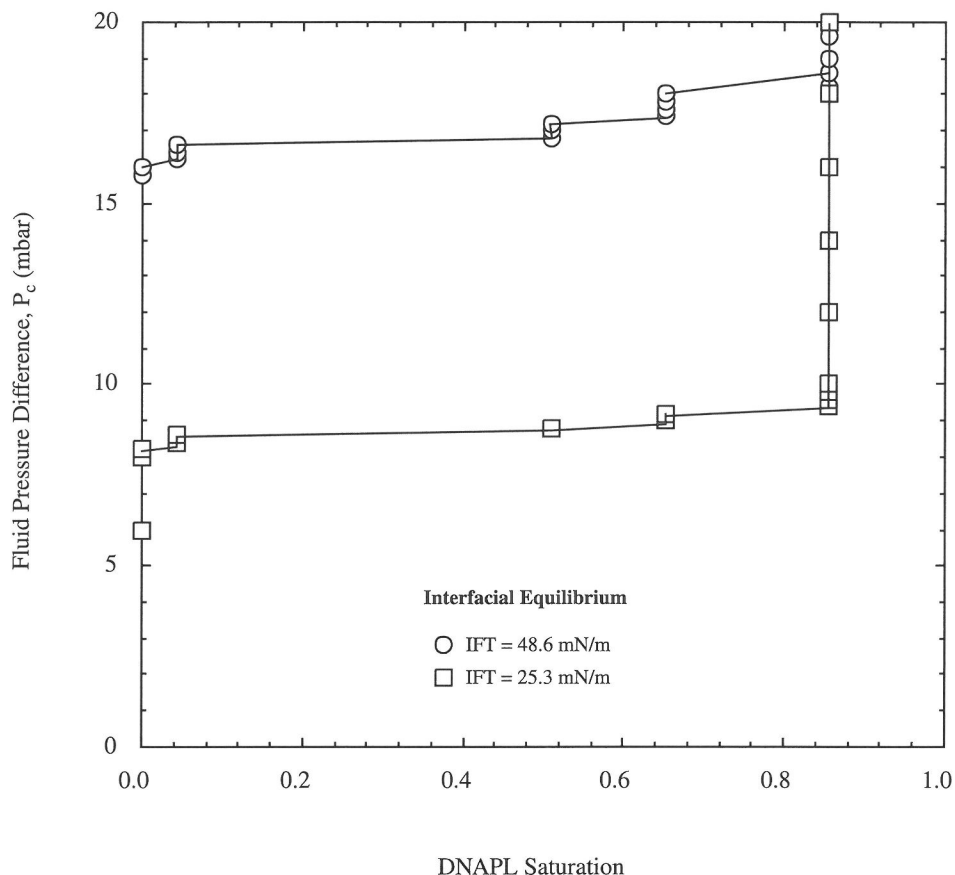


Fig. 7. Pore-scale model results using single-valued ("equilibrium") interfacial tension. The interfacial tension between pure PCE and water is 48.6 mN/m; note the entry pressure at approximately 16 mbars.

was incorporated in these experiments. Maximum saturation varied under the different applied capillary pressures in a non-monotonic fashion (see Fig. 9). Maximum saturation ranged from 0.8542 to 0.9894. A minimum value for the maximum saturation was obtained under the 17-mbar and 18-mbar capillary pressure conditions, i.e., those constant capillary pressure conditions just above the entry pressure for pure PCE. The slopes of the curves illustrate that time was an important variable in reaching the final saturation. The locations of the curves along the time scale indicate that drainage occurs more quickly under the higher applied capillary pressure conditions. Three different NAPL migration rates were calculated for each experiment from the saturation histories in the bottom row of pores. The rates were based on the average distance from the non-wetting phase reservoir to the bottom row of pores and on three different "arrival" times: first arrival of NAPL,

the interpolated time when NAPL saturation reached 0.5, and the time when NAPL saturation reached 1.0. These rates are shown as a function of the constant capillary pressure in Fig. 10.

3.3. Discrete Pressure-Step Increments

Model results for the third set of experiments are presented in Fig. 11, where they are presented in comparison to the results in which single, "equilibrium" values of interfacial tension were assumed. Capillary pressure at which NAPL first enters the medium decreased and the maximum saturation attained in an experiment increased as the equilibration time was increased between pressure increments. Maximum saturation is shown as a function of the pressure-step equilibration time in Fig. 12. Maximum saturation in these experiments ranged between 0.8703 and 0.9504.

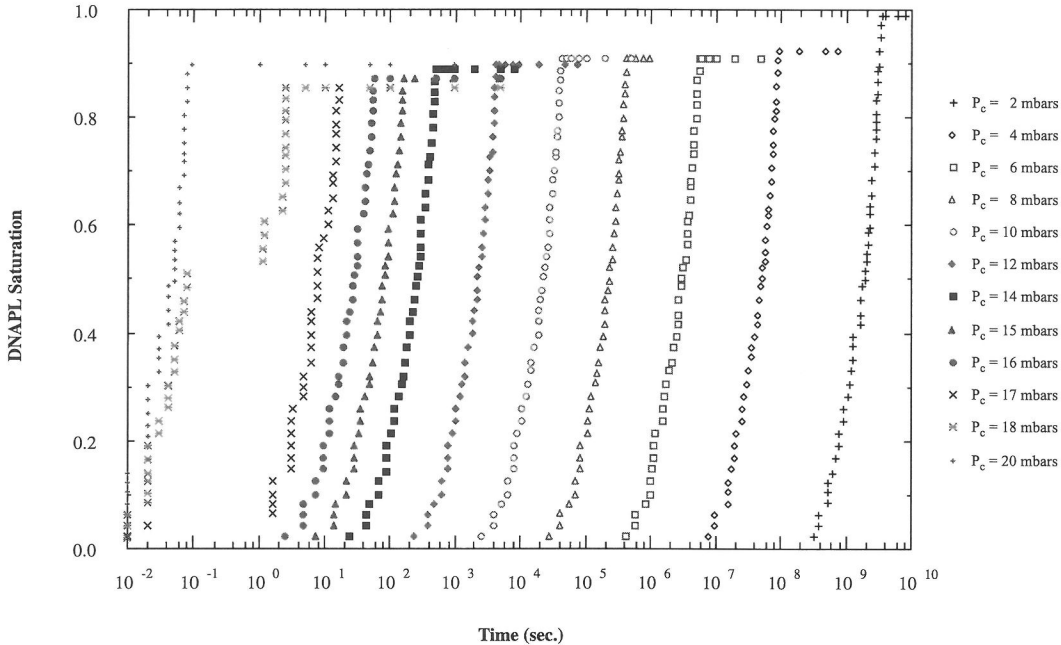


Fig. 8. Pore-scale model results with time-dependent interfacial chemistry incorporated. Saturation becomes a function of time as well as applied capillary pressure.

4. DISCUSSION

4.1. Equilibrium Interfacial Tension

Results from the first set of experiments are consistent with typical results from uniform grain-size porous media. The rapid increase in PCE saturation reflects the near homogeneity of this medium. The rapid build-up of PCE saturation occurs between capillary pressures of 16 and 18 mbars for pure PCE ($\gamma_{nw} = 48.6$ mN/m) and between 8 and 9 mbars for the lower assumed interfacial tension value (25.3 mN/m). All of the PCE saturation occurs in the coarser pores surrounding the finer pore domain. These results are consistent with those reported by Ferrand and Celia (1992). Irreducible wetting phase saturation is determined by the finer pore-throat heterogeneity embedded within the model. Results for the lower “equilibrium” interfacial tension are consistent with the standard assumption of Leverett J-function scaling of capillary pressure saturation curves based on changing the interfacial tension between the fluids (Leverett, 1941; Bear, 1972). The capillary pressure-saturation curve is mere-

ly shifted to lower capillary pressures in response to the lower interfacial tension. These results confirm that the model is a reasonable approximation of a real porous medium, and that it demonstrates behavior comparable to pore-scale simulations in which a much greater number of pores were used and the standard assumptions of equilibrium interfacial chemistry were employed (Ferrand and Celia, 1992).

4.2. Time-Dependent Interfacial Tension

There are several things to note in Fig. 8. First, there are discrete discontinuities in the S_{PCE} -time curves. This is especially apparent in the P_c - S_{PCE} curve for 18 mbars. These discontinuities occur when multiple pore throats become unstable simultaneously. To some extent the apparent discontinuities are an artifact of the model since discrete categories of pore throat sizes were used rather than a smooth distribution, and also, because of the small total number of pores. This result is physically reasonable, however, as Haines jumps can occur simultaneously through many different pores in real porous media (Payatakes,

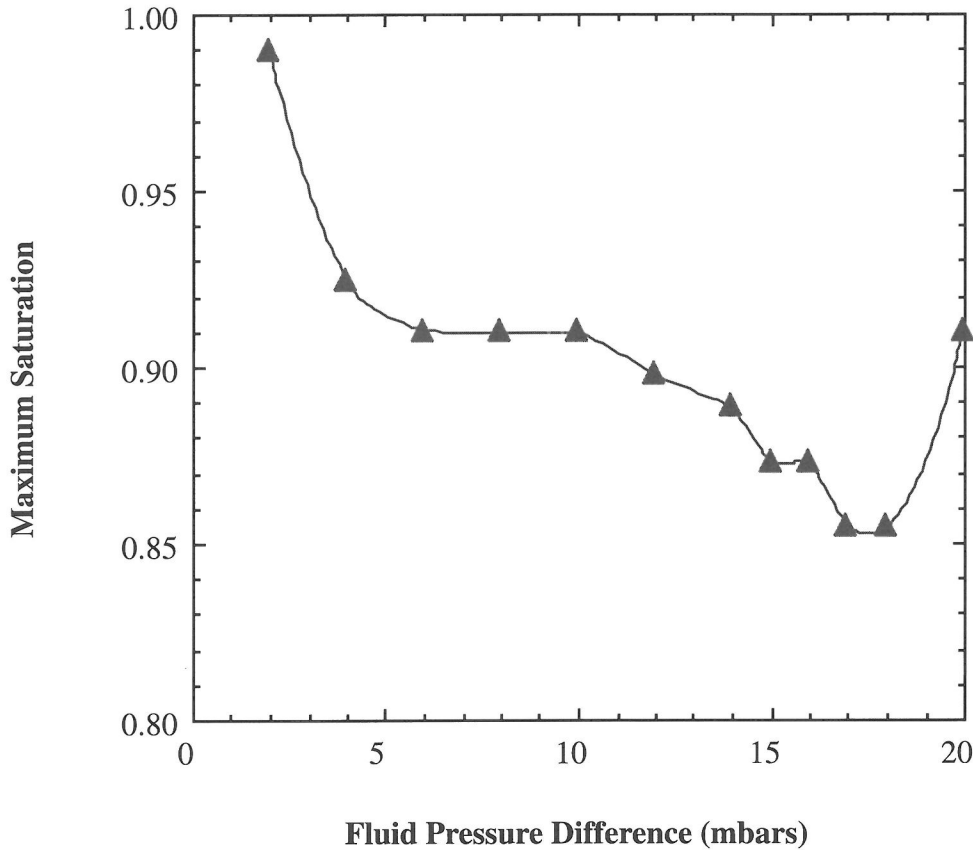


Fig. 9. Maximum NAPL saturation as a function of applied capillary pressure with interfacial chemical kinetics incorporated in the pore-scale model. Maximum saturation occurs at a pressure significantly lower than the entry pressure for the pure bulk NAPL with no interfacially-active component.

1982). It also happens when an interface jumps through multiple pore bodies because the pore throat radius at the end of the first pore body being “jumped” (or subsequent pores “jumped”) is not sufficiently small to establish a stable interface and therefore stop its advance (Payatakes, 1982). Heller’s (1968) movie-frames of 1,1,1-trichloroethane drainage that show Haines jumps covering several to several tens of pores provide visual experimental documentation that this occurs.

The second thing to note is that the non-wetting phase saturation, S_n , becomes a function of both capillary pressure and time, with the time-dependence arising through the interfacial chemical kinetics:

$$S_n = S_n(P_c, t) \quad (11)$$

The time-dependence enters from the time-dependent surface chemistry at capillary pressures below the

entry pressure for pure PCE and from a combination of viscous flow and the time-dependent surface chemistry at capillary pressures above the pure PCE entry pressure. The time scale varies as a function of the capillary pressure boundary conditions. However, non-wetting phase penetration of the medium does not necessarily stop at a threshold capillary pressure, as applied by Leverett (1941). Leverett’s work presupposes equilibrium interfacial chemistry, and hence a threshold capillary entry pressure for the medium/fluid combination. The threshold entry pressure becomes somewhat nebulous under the conditions of time-dependent surface chemistry. Penetration of the medium still occurs in the combination modeled here, even at capillary pressures significantly below the “threshold” pressure for undyed PCE. NAPL penetrates the medium at different rates. The penetration or migration rate is a function of the boundary fluid pressure difference. However, penetration or migration of NAPL does not

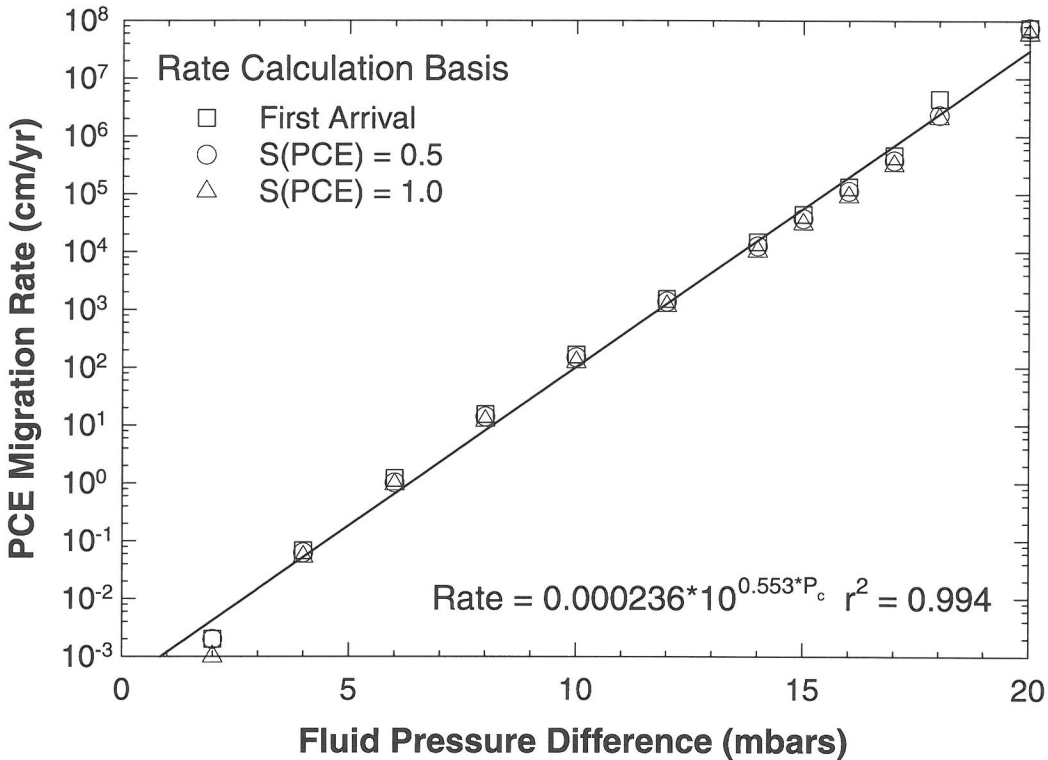


Fig. 10. NAPL migration rate as a function of applied capillary pressure with interfacial chemical kinetics incorporated in the pore-scale model.

stop at fluid pressure differences below the “threshold” capillary pressure, assuming equilibrium interfacial tension. These rates are more a function of the non-linear chemical kinetics than of the capillary pressure. The approximate log-linear curve reflects the log-linear nature of the interfacial chemistry time dependence given by Eqn. 9.

The third and very important, although rather obvious, observation is that penetration of a porous medium occurs at capillary pressure boundary conditions lower than those predicted by the standard equilibrium capillary pressure-saturation model, *if static values are assumed for interfacial tension and contact angle which are higher than the true equilibrium values*. This is important to bear in mind when interpreting multiphase flow visualization experiments in which NAPLs dyed with azo dyes are used. These dyes have generally been assumed to have no effect on the interfacial chemistry. The work of Tuck and coworkers (Tuck et al., 1998; Tuck and Rulison, 1999b), as illustrated in Figs. 4 and 5, demonstrates that this assumption is inappropriate.

The fourth, and perhaps most intriguing observation, is that maximum nonwetting phase saturation, $S_{n, max}$, may not increase monotonically with capillary pressure, as the standard, equilibrium capillary pressure-saturation model predicts. This is illustrated in Fig. 9. In fact, lower maximum NAPL saturation occurred at fluid reservoir pressure differences near the entry pressure for the equilibrium capillary pressure-saturation model for the pure solvent, in this specific case approximately 16 mbars. This minimum appears to arise from competition between whether the capillary pressure boundary values or the time-dependent surface chemistry will determine whether a given pore is penetrated or not. Near the entry pressure for the medium, the capillary pressure and time-dependent surface chemistry play nearly equal roles in determining when and which pores become filled with NAPL. The capillary pressure is the dominant control at higher capillary pressure boundary values. Alternatively, the time-dependent chemistry dominates control of when and whether a given pore will become filled at

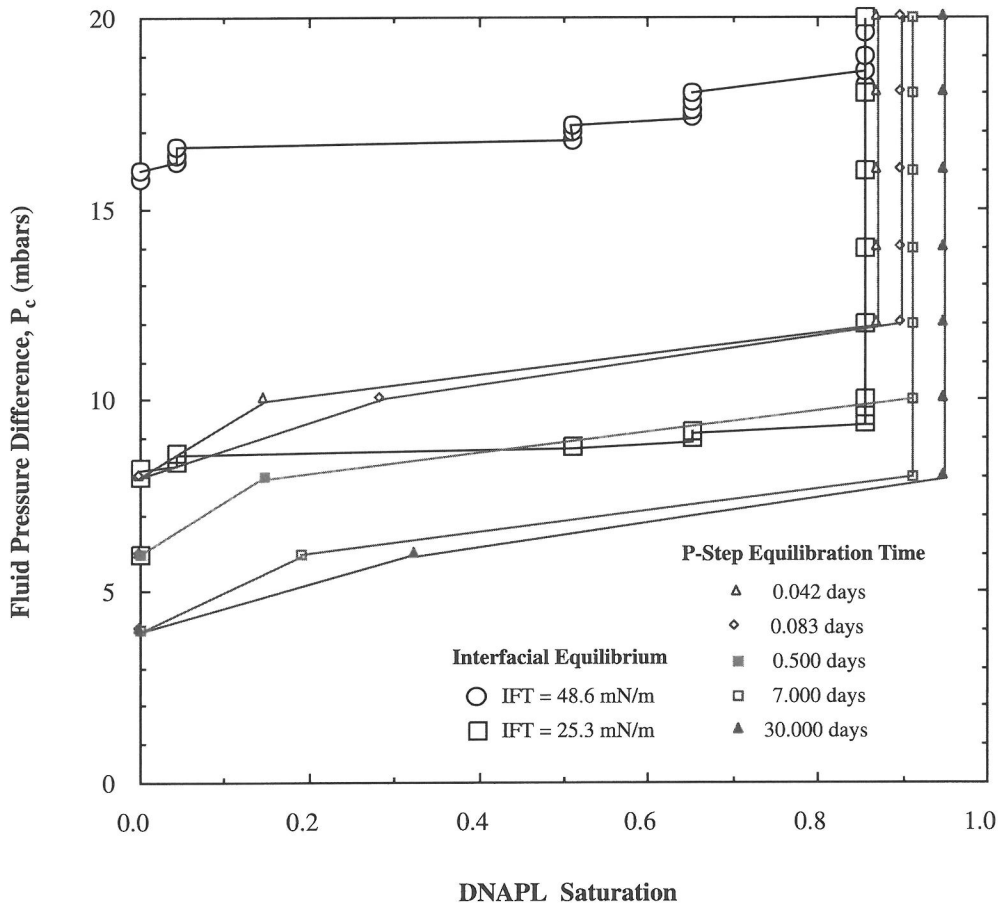


Fig. 11. Pore-scale model results for incremented pressure-step experiments under conditions of time-dependent interfacial tension as a function of pressure-step equilibration time.

capillary pressures below the entry pressure for a pure, single-component NAPL (in this case, PCE) with no surface-active components.

An analysis of variance was performed to test whether or not the minimum saturations were significant. The actual entry pressure for undyed PCE was 16.04 mbar. Four experiments were run in which the difference between this entry pressure and the modeled pressure was less than 2 mbars. Those experiments also yielded the lowest values for $S_{n,max}$. These were thus assigned to one group, having four samples. The remaining experiments, with the exception of the $P_c = 2$ mbar, were assigned to a second group, resulting in a subtotal of 7 experiments. A model II analysis of variance was performed to test the null hypothesis that the mean saturation values for both groups are equal (Sokal and Rohlf, 1969). The experiment F-statistic was 40.16. The critical value of the

F-distribution for $p=0.001$ with the Among Groups degrees of freedom equal to one ($df = 1$) and the Within Groups degrees of freedom equal to nine ($df = 9$) is 22.9 ($F_{0.001[1, 9]} = 22.9$, Rohlf and Sokal, 1969). Thus, the two groups have statistically different means ($p < 0.001$), i.e., the minimum in the plot of S_{max} vs. P_c is statistically significant. The maximum NAPL saturations for boundary fluid pressure differences within ± 2 mbar of the pure-solvent equilibrium entry pressure are statistically significantly lower than maximum NAPL saturations for boundary fluid pressure differences outside this range.

4.3. Discrete Pressure-Step Increments

The results of the third set of experiments (Fig. 11), those in which the fluid reservoir pressure difference was incrementally ramped up, provide a qualitative

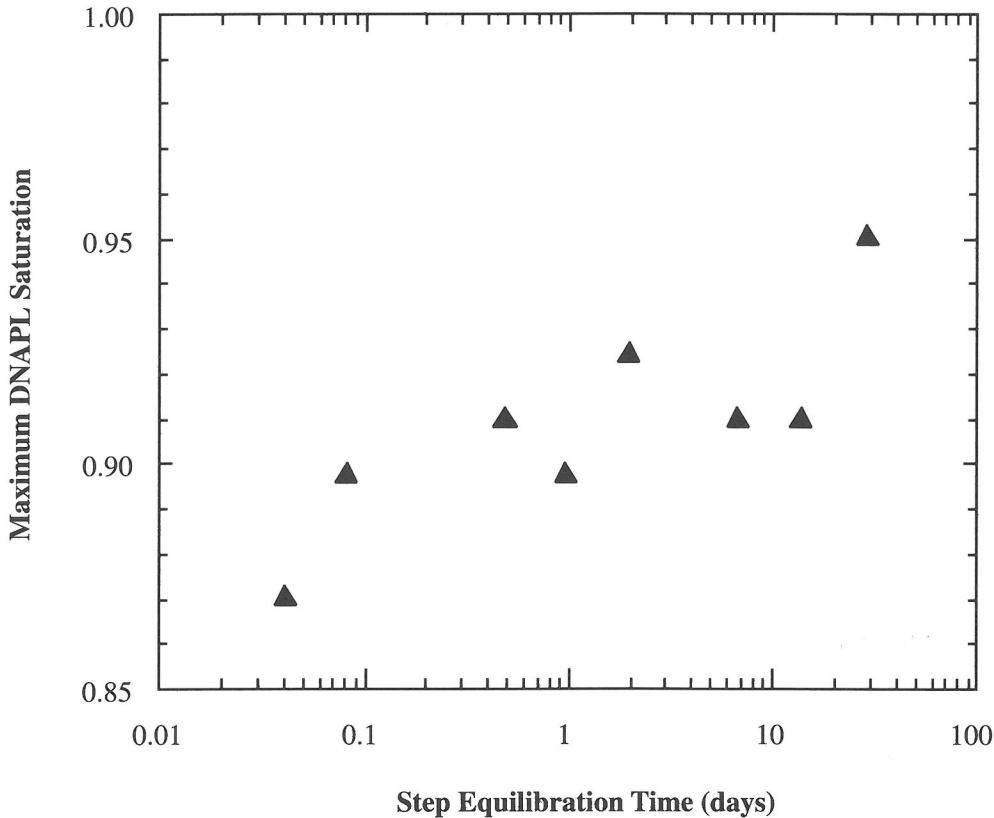


Fig. 12. Maximum saturation as a function of the pressure-step equilibration time.

view of the effects that time-dependent surface chemistry would be expected to have on current experimental techniques for measuring the capillary pressure-saturation relationship. The results suggest, depending on the time used for equilibration between pressure increments, that we could expect measured results to approximate those based on simply assuming the equilibrium interfacial tension for the dyed PCE-water system, with the caveat that we would expect to see higher final PCE saturation. But this is very deceptive. In fact, what we would more likely see is that our current experimental approach using a real porous medium sample would yield a curve somewhere between that of undyed PCE and the equilibrium-interfacial tension curve. The difference between what the current model results suggest and what we would actually measure arises from the extremely small sample of porous medium represented by this model.

We can begin to understand why this is so by thinking about what would happen if the model domain were expanded by simply linking multiple copies of the current 7×7 pore-scale model. We would obtain nearly the same results if we expand the model domain only in the direction transverse to flow. If, on the other hand, we were to expand the model domain in the direction parallel to flow, the results would be much different. The reason for this is that rates of PCE migration are slow at pressures below the entry pressure for undyed PCE (see Fig. 10). A low migration rate results in a relatively higher saturation in the short model because it can still cover an appreciable fraction of the model domain. Low migration rates under the low fluid pressure differences would penetrate a progressively lower fraction of the model as the length of the domain increased in the direction parallel to flow. A "standard" capillary pressure-satu-

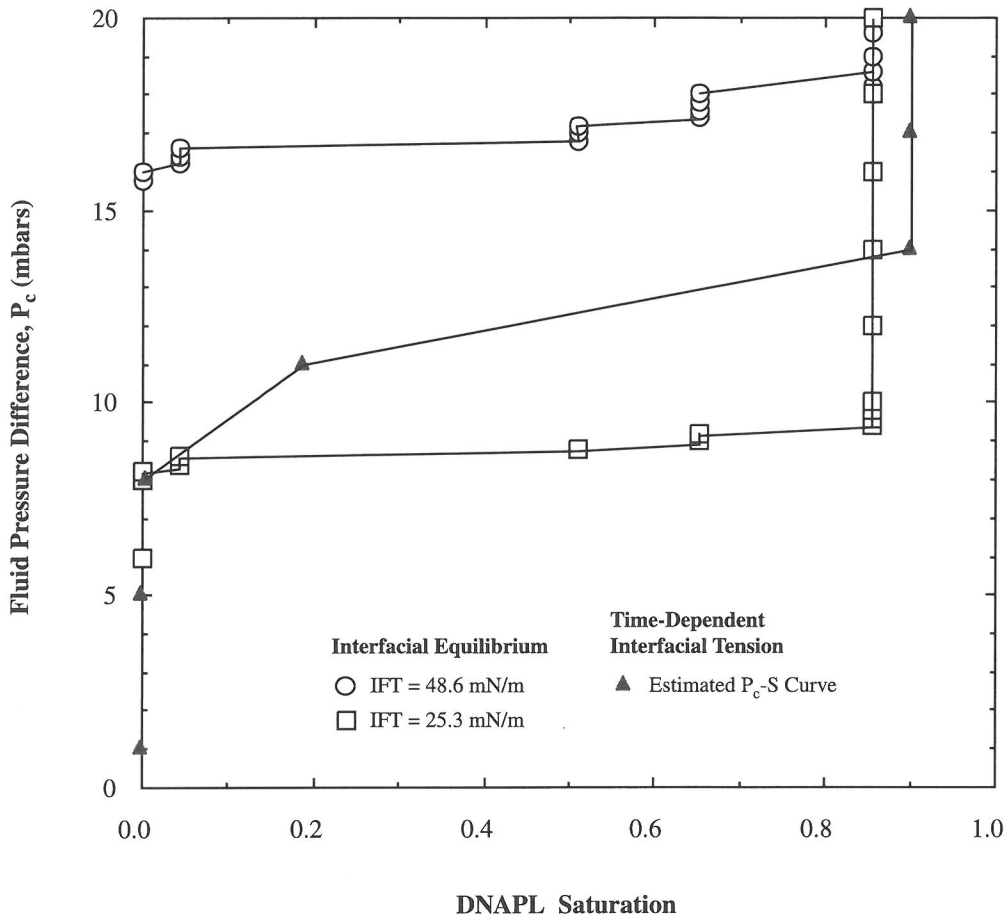


Fig. 13. Estimated capillary pressure-saturation curve for a 7.5 cm long, 2-D medium composed of linked copies of the 7x7 pore-scale model presented here. Saturation was approximated based on the fraction of the medium covered in a pressure-increment/time-step using the migration rates presented in Fig. 10. Bounding "equilibrium" interfacial tension curves for the 7x7 model are shown for comparison.

ration curve, as we would measure it in a Tempe cell, can be estimated using the following approximation:

$$S_{est}(P_c) = \left(\frac{D_{mig}}{D_{cell}} \right) S_{max} \quad (12)$$

where $S_{est}(P_c)$ is the estimated saturation at a fluid reservoir pressure difference of P_c , D_{mig} is the estimated distance PCE would migrate during the pressure-step equilibration time, D_{cell} is the length of the Tempe cell, and S_{max} is the estimated maximum saturation. D_{mig} can be estimated using the following relation:

$$D_{mig} = R_{mig}(P_c) \left(\frac{\Delta t}{365} \right) \quad (13)$$

where $R_{mig}(P_c)$ is the migration rate as a function of the boundary fluid pressure difference estimated from

the exponential curve fit in Fig. 10 and Δt is the pressure-step equilibration time in days. This approach yields an approximate capillary pressure-saturation relationship for the 2-D model domain based on the fractional length of porous medium covered during a pressure-increment/time-step, as determined by the migration rates of Fig. 10.

Common practice in geotechnical companies is to measure the capillary pressure-saturation relationship using seven pressure levels over a two-week period, i.e., an average equilibration time of 2 days. Fig. 13 contains the estimated capillary pressure-saturation relationship for this Tempe-cell model domain based on the fraction of the porous medium covered during a pressure-increment/time-step as determined by the migration rates of Fig. 10. I assumed a Tempe cell length of 7.5 cm (3 inches),

0.9 for S_{max} , and the following sequence of pressures: 1 mbar, 5 mbar, 8 mbar, 11 mbar, 14 mbar, 17 mbar, and 20 mbar. The estimated curve falls between the bounding curves generated assuming single-values for the interfacial tension. Even this estimated curve is probably biased toward the curve for the lower interfacial tension. The reason is that the oil-wetted pressure plate used to separate the oil reservoir from the porous medium would likely adsorb a significant amount of any surface active component before it got into the medium. Hence, the current experimental technique is likely to bias results toward higher interfacial tension than what may actually occur in a "real" setting.

4.4. Model Limitations

4.4.1. Model size

Clearly, a major criticism of this model can be leveled at the paucity of its size. I believe the results to be valid, however, for several reasons. First, it demonstrates the qualitative behavior observed in standard capillary pressure-saturation measurements made in real porous media consisting of narrow grain size, hence pore size, distributions (see Fig. 7). Rapid water drainage occurred over a narrow range of capillary pressure once the critical capillary pressure was exceeded. The model also illustrates the concepts of by-passing and stranding of water in the finer pores. Hence residual water saturation was observed. This result is comparable to those of Ferrand and Celia (1992) who used a much larger number of pores in their simulations. In addition, the results with respect to NAPL-front penetration rate are qualitatively similar to the model results of Giordano and Slattery (1983a; 1987) for one-dimensional displacement rates of discontinuous NAPL in capillary tubes in which they explicitly incorporated interfacial viscosity (i.e., time-dependent surface chemistry).

4.4.2. Interfacial chemistry time-dependence

Another criticism of the model can be leveled against the representation of the interfacial tension time-dependence. The logarithmic equation implies that interfacial tension can decrease infinitely, including reaching negative values at sufficiently large time. This is clearly a physical impossibility. The interfacial tension eventually reaches a stable equilibrium or meso-equilibrium value, rather than continuing to decline. A better representation of this time-dependence would be that due to Hua and Rosen (1988). They represented the time dependence of dynamic surface tension using the following equation:

$$\gamma_t - \gamma_m = \frac{\gamma_o - \gamma_m}{1 + \left(\frac{t}{t^*}\right)^n} \quad (14)$$

where γ_t is surface or interfacial tension at time t , γ_o is the surface or interfacial tension of the pure solvent, γ_m is the meso-equilibrium surface or interfacial tension, and t^* and n are constants. This equation captures the approach of surface or interfacial tension to an equilibrium or meso-equilibrium value and the observations that time-dependent interfacial tension rarely exceeds that of the pure, bulk solvent. This form could easily be incorporated into the model if sufficient data were available. Currently there are insufficient time data for the system modeled here to have reached meso-equilibrium.

Tuck and Rulison (unpublished data) monitored the interfacial tension in the system modeled here out beyond eight hours (>28,800 sec). Interfacial tension continued to decline log-linearly for this whole time following Eqn. 9 and showed no trend that the log-linear phase of the decline was nearing. Similarly, they followed the contact angle for more than 30 days (2.592×10^6 sec). Again, the contact angle continued to follow the log-linear trend of Eqn. 10 with no sign of deviation. Comparison of these experimental times with the critical ages illustrated in Fig. 6 reveals that the contact angle data fall within the majority of the modeled time-scales, but the modeled interfacial tension implies an extrapolation of the experimentally measured data. Only pore-throats down to category 6 (see Table 2), however, were ever invaded in the model, with the exception of the experiment with constant capillary pressure of 2 mbar (2 mbar results). Thus, the actual maximum time any NAPL-water interface spent in a specific pore-throat (i.e., the maximum interface age used in the modeling) was 204,700 seconds, again with the exception of the 2 mbar results. Extrapolation of the interfacial tension data presents no problem if we assume that the contact angle behavior is indicative of what the interfacial tension behavior would be, i.e., that the log-linear rate of decrease would continue beyond 30 days. The log-linear equations for the interfacial tension and contact angle still give physically reasonable values well beyond the time frames discussed here. Thus, there is no conflict at all if the interfacial chemical kinetics are viewed as purely arbitrary, and not meant to model a specific system. This might be very reasonable in the geologic time regime characteristic of primary oil migration. In that case, surface-active components will migrate at different rates than the bulk oil due to adsorption loss on mineral surfaces. This could significantly retard the surface chemical kinetics at the leading edge of the migrating oil.

4.4.3. Interface age

Another limitation of this model is that the effective age of an interface gets reset essentially to zero after each Haines jump in order to directly apply the interfacial chemical kinetics of Eqn. 9. The interfaces measured via the drop volume technique start from a “fresh” condition since they arise from the break occurring when a drop falls from the measurement instrument (see Tuck and Rulison, 1999b, for details). Interfaces in a porous medium do not form in this fashion during drainage. Instead, they go through cycles of dilation and contraction, as illustrated in Fig. 1.

An “effective” age of the “fresh” interfaces can be defined in terms of the initial interfacial surface excess, Γ_3^σ , when a quasi-stable interface is first formed following a Haines jump. A rigorous model of the concepts involved in this paper would entail modeling the surface expansion and subsequent change in interfacial excess, Γ_3^σ , as an interface makes a Haines jump and establishes its new “stable” positions in the subsequent pore throats. A relatively simple approximation of this effect can be made by proportionately reducing the interfacial excess in effect when an interface reaches the narrow-point of the pore throat, as illustrated in Fig. 1c. The factor for the reduction will be approximated by the ratio of the interfacial area in the pore-throat just before a Haines jump occurs to the sum of the new interfacial areas established in the subsequent pore-throat after completion of the Haines jump. The justification for this approximation lies in the direct relationship between interfacial tension reduction and the surface excess as expressed in Eqn. 3. This approach leads to the following equation to estimate the initial interfacial tensions of the “fresh” interfaces in this model:

$$\gamma_{t=0} = \gamma_o \left(1 - \frac{\frac{1}{3} \Gamma_3^\sigma \mu_3}{\gamma_o} \right) \quad (15)$$

where γ_o is the interfacial tension of the pure NAPL or solvent, and $\gamma_{t=0}$ is the adjusted interfacial tension for the “fresh” interfaces in the porous medium following a Haines jump. This approach assumes: 1) that the new interfaces are established simultaneously, 2) that the areas of the new interfaces are all identical or at least negligibly different, and 3) that the surface excess just before the Haines jump is distributed equally over the new interfaces.

4.5. Experimental Support

Tuck and co-workers (Pirkle et al. 1997a,b; Tuck et al., 2000) conducted experiments to test the role of time-dependent surface chemical effects on Sudan IV-dyed PCE displacement of water using glass bead

porous media. In their early work (Pirkle et al., 1997a), they measured the entry pressures of PCE with various Sudan IV dye concentrations in uniform glass bead porous media. Each experiment from that work lasted less than eight hours. They measured an entry pressure of 15.45 cm of PCE with a standard deviation of 0.66 cm (n=4) for the dye concentration used in the model results reported here. This translates to an expected capillary entry pressure of 24,500 baryes (g/cm-sec^2). The 95% confidence interval for the entry pressure of PCE with this dye concentration in this medium was thus 13.35 to 17.55 cm of PCE (21,200 to 27,900 baryes). In a later experiment (Pirkle et al., 1997b; Tuck et al., 2000), they set a dyed PCE column above a water-saturated glass bead medium of the same grain size to a height of approximately 9 cm, and then monitored the experiment for nearly 70 days. Thus, the surface chemical time-dependence became the primary variable governing penetration of the glass bead medium in the latter experiment since the target fluid pressure difference was less than 60% of the expected entry pressure and less than 70% of the lower 95% confidence limit for entry pressure. They saw visual penetration of the medium to a depth of approximately 2 mm. They also noted that the glass beads in this top 2 mm section of the column had become stained red by the Sudan IV dye. Limitations of their experimental apparatus, however, allowed a spike in capillary pressure that exceeded the lower 95% confidence limit, but did not exceed the mean entry pressure measured previously. Thus, their results, at this time, offer only qualitative evidence supporting the theory and model presented here. Further experimental work is needed.

4.6. Model Implications

The major conceptual advance of this work is to incorporate time explicitly into the capillary pressure-saturation relationship via incorporation of time-dependent surface chemistry. The result is that the rate of advance of a NAPL front during primary drainage can be estimated from this type of model. Following the multi-scale model concept of Celia et al. (1993), embedding such a pore-scale model into a continuum model might thus allow more accurate estimation of NAPL migration rates and be used to help determine time step length for the continuum-scale model component.

An additional connection to continuum-scale behavior arises from the interaction between the interfacial chemical kinetics and the porous medium heterogeneity. The model results imply that this interaction may determine the portion of finer pore-size heterogeneities that are by-passed during primary drainage. This inter-

play will be a function of the applied capillary pressure and the magnitude of the heterogeneity, as well as the interfacial chemical kinetics.

The use of equilibrium interfacial tensions will lead to overestimating the rate of NAPL migration in models involving complex fluids containing interfacially active components. This will be especially true for situations where the capillary pressure is relatively low.

The interfacial chemistry changes occur due to adsorption and partitioning of interfacially active components to the fluid-solid and fluid-fluid interfaces as discussed above. Equation 3 indicates that the magnitude of the equilibrium change in interfacial tension is directly proportional to the chemical activity of the surface-active component. Thus, the magnitude and rate of interfacial tension decline and contact angle increase will change with long-term migration as the interfacially active component(s) is (are) lost by adsorption onto the porous medium solids. This should have the effect of decreasing the rate of NAPL migration as it moves away from the source area. This effect may have particular relevance to primary migration of oil out of a source rock toward a trap since these distances are on the scale of geologic basins, as opposed to tens to hundreds of meters at a contaminated site.

Current experimental techniques for measuring the capillary pressure-saturation relationship are likely to cause significant inaccuracy for complex NAPLs containing surface active components. This arises from the interplay of the time-dependent chemical kinetics, the applied fluid reservoir pressure difference, the resulting rate of NAPL migration, and the length of the pressure-step equilibration time.

5. CONCLUSIONS

Surface chemical kinetics is a well-established phenomenon in multicomponent fluid systems. Time-scales for interfacial tension change range from milliseconds to hours, and even days and longer, while those for contact angles can range up to months and perhaps longer, depending on the system. *A priori* assumption of equilibrium values for interfacial tension and/or contact angle may not be appropriate since most systems of practical interest, whether experimental or field situations, involve such multicomponent systems.

Whether or not dynamic surface chemistry must be considered depends on three issues. The first is whether or not a surface-active component is present in the system of interest. The equilibrium assumption is perfectly valid for simple, two-component systems involving pure bulk fluids. In field situations and in laboratory systems in which dyes are used to aid

visualization, the equilibrium assumption needs to be examined. The second issue concerns the relative time scales of the process under consideration and the specific dynamic surface chemical kinetics of the system involved. Any process involving interfacial dilation or compression that occurs on a time-scale significantly shorter than the time-scale of the surface chemical kinetics should be evaluated for the need to incorporate the kinetics. Primary drainage in a porous medium of a multicomponent, non-wetting liquid (for example, a complex NAPL in water-wetted media) containing a surface-active component is a process for which the interfacial chemical kinetics should be evaluated. The third issue is whether the magnitude of the interfacial property changed is great enough to significantly alter the process, i.e., are the concentration and surface chemical behavior of a surface active species sufficient to produce significantly different capillary behavior.

The results of incorporating interfacial kinetics in a pore-scale model illustrate its importance. Contrary to the standard, equilibrium capillary pressure-saturation measurement procedures, the attainment of "equilibrium" may take far longer than ordinary laboratory time-scales. The non-wetting phase saturation becomes a function of both the capillary pressure (the traditional view) and the surface chemical kinetics under these conditions. The rate of migration of a NAPL front becomes a function of the interfacial chemical kinetics. Maximum NAPL saturation can no longer be seen as a monotonically increasing function of the capillary pressure boundary conditions alone. Rather, in pore-scale heterogeneous media at least, competition between whether the capillary pressure boundary conditions or the interfacial chemical kinetics are more important for determining when and if an interface advances result in a minimum in a plot of maximum NAPL saturation versus capillary pressure. The minimum occurs near the entry pressure for the pure bulk fluid without surface active components.

Current experimental techniques for measuring the capillary pressure-saturation relationship can mask the effects of time-dependent surface chemistry through both large pressure increments and short equilibration times. In addition, it is likely that oil-wetted pressure-plates could remove significant amounts of surface-active components in a NAPL prior to its encountering the test medium.

The effects of modeling multiphase flow by assuming equilibrium values for interfacial properties will be to over-estimate the rate at which a NAPL front advances, particularly at capillary pressures which just exceed the entry pressure for the medium. Another effect will be to underestimate the time

required for NAPL to penetrate finer-grained units. In addition, it is likely that NAPL saturation may be off by a significant amount. More detailed work is needed to verify the results presented here. Both experimental and more elaborate modeling are warranted to test the predictions.

Acknowledgements—It is with great pleasure that I thank Dr. Roland Hellmann and Dr. Scott Wood for arranging this special issue honoring Dave Crerar. Dave was instrumental in bringing me to Princeton and connecting me with my subsequent advisor, mentor, and colleague, Peter Jaffe, Professor of Civil Engineering, Princeton University. It is, of course, impossible to say what my career would have looked like without this connection, but I doubt that it would have been as rich in intellectual stimulation. Dave's rapid decline in health, having occurred during my time at Princeton, was a great loss. Dave's capabilities and knowledge, at what should have been the height of his productivity, would have been an even greater blessing than Peter's alone.

I wish to acknowledge Dr. Roland Hellmann of the Univ. of Grenoble, Dr. Jonathan C. Johnson of the USGS, Dr. Tissa Illangasekare of the Colorado School of Mines, and an anonymous reviewer for their comments on the paper. They greatly improved its content and presentation. I also wish to thank Westinghouse Savannah River Co. and the U.S. Department of Energy, who have both directly and indirectly supported the work which forms the foundation of this paper.

Editorial handling: R. Hellmann

REFERENCES

- Adamson A.W. (1990) *Physical Chemistry of Surfaces*, 5th ed. John Wiley & Sons Inc., New York.
- Addison C.C. and Litherland D. (1953) The properties of freshly formed surfaces. Part XVIII. Dynamic surface potentials and the adsorption process: Molecular orientation in soluble films of decyl alcohol. *J. Chem. Soc.* 1143-1150.
- Andreas J.M., Hauser E.A., and Tucker W.B. (1938) Boundary tension by pendant drops. *J. Phys. Chem.* **42**, 1001-1019.
- Bear J. (1972) *Dynamics of Fluids in Porous Media*. American Elsevier Publishing Company, Inc., New York.
- Bigelow S.L. and Washburn E.R. (1928) Variations in the surface tensions of solutions. *J. Phys. Chem.* **32**, 321-353.
- Blunt M. and King P. (1991) Relative permeabilities from two- and three-dimensional pore-scale network modeling. *Transp. Porous Media* **6**, 407-433.
- Bohr N. (1909) Determination of the surface-tension of water by the method of jet vibration. *Philos. Trans. Royal Soc. (London) A* **209**, 281-317.
- Boussinesq M.J. (1913) Sur l'existence d'une viscosité superficielle, dans la mince couche de transition séparant un liquide d'un autre fluide contigu. *Ann. Chim. Phys.* **8^e Série**, **29**, 349-357.
- Brewster M.L., Annan A.P., Greenhouse J.P., Kueper B.H., Olhoef G.R., Redman J.D., and Sander K.A. (1995) Observed migration of a controlled DNAPL release by geophysical methods. *Ground Water* **33**, 977-987.
- Catino S. and Farris R.E. (1978) Azo dyes. In *Kirk-Othmer Encyclopedia of Chemical Technology* (eds. H.F. Mark, D.F. Othmer, C.G. Overberger, and G.T. Seaborg). John Wiley & Sons, New York. pp. 387-433.
- Celia M.A., Rajaram H., and Ferrand L.A. (1993) A multi-scale computational model for multiphase flow in porous media. *Adv. Water Resour.* **16**, 81-92.
- Celia M.A., Reeves P.C., Ferrand L.A. (1995) Recent advances in pore-scale models for multiphase flow in porous media. *Reviews Geophysics*, Supplement, "U.S. National Report to the Union of Geodesy and Geophysics 1991-1994", 1049-1057.
- Crawford F.W. and Hoover G.M. (1966) Flow of fluids through porous mediums. *J. Geophys. Res.* **74**, 2911-2917.
- Dullien F.A.L. (1992) *Porous Media: Fluid Transport and Pore Structure*, 2nd ed. Academic Press, Inc., San Diego.
- Dupré A. (1869) *Théorie Mécanique de la Chaleur*. Gauthier-Villars, Paris.
- Ferrand L.A. and Celia M.A. (1992) The effect of heterogeneity on the drainage capillary pressure-saturation relation. *Water Resour. Res.* **28**, 859-870.
- Fortin J., Jury W.A., and Anderson M.A. (1997) Enhanced removal of trapped non-aqueous phase liquids from saturated soil using surfactant solutions. *J. Contam. Hydrol.* **24**, 247-267.
- Gibbs J.W. (1948) *The Collected Works of J. Willard Gibbs. Vol. I. Thermodynamics*. Yale University Press, New Haven.
- Giordano R.M. and Slattery J.C. (1983a) Effect of interfacial viscosities upon displacement in capillaries with special application to tertiary oil recovery. *A.I.Ch.E. J.* **29**, 483-492.
- Giordano R.M. and Slattery J.C. (1983b) Stability of static interfaces in a sinusoidal capillary. *J. Colloid Interface Sci.* **92**, 13-24.
- Giordano R.M. and Slattery J.C. (1987) Effect of interfacial viscosities upon displacement in sinusoidal capillaries. *A.I.Ch.E. J.* **33**, 1592-1602.
- Graton L.C. and Fraser H.J. (1935) Systematic packing of spheres with particular relation to porosity and permeability. *J. Geol.* **43**, 785-909.
- Haines W.B. (1930) Studies in the physical properties of soil. V. The hysteresis effect in capillary properties, and the modes of moisture distribution associated therewith. *J. Agric. Sci.* **20**, 7-116.
- Heller J.P. (1968) The drying through the top surface of a vertical porous column. *Soil Sci. Soc. Am. Proc.* **32**, 778-786.
- Hua X.Y. and Rosen M.J. (1988) Dynamic surface tension of aqueous surfactant solutions I. Basic parameters. *J. Colloid Interface Sci.* **124**, 652-659.
- Kueper B.H. and Frind E.O. (1991) Two-phase flow in heterogeneous porous media 2. Model application. *Water Resour. Res.* **27**, 1059-1070.
- Leverett M.C. (1941) Capillary behavior in porous solids. *Pet. Trans., A.I.M.E.* **142**, 152-169.
- Lucassen J. and Giles D. (1975) Dynamic surface properties of nonionic surfactant solutions. *J. Chem. Soc., Farad. Trans.* **71**, 217-232.
- Melrose J.C. (1965) Wettability as related to capillary action in porous media. *Soc. Pet. Eng. J.* **5**, 259-271.
- Miller E.E. and Miller R.D. (1956) Physical theory for capillary flow phenomena. *J. Appl. Phys.* **27**, 324-332.
- Morrow N.R. (1971) Small-scale packing heterogeneities in porous sedimentary rocks. *A.A.P.G. Bull.* **55**, 514-522.
- Pan R., Green J., and Maldarelli C. (1998) Theory and experiment on the measurement of kinetic rate constants for surfactant exchange at an air/water interface. *J. Colloid Interface Sci.* **205**, 213-230.

- Payatakes A.C. (1982) Dynamics of oil ganglia during immiscible displacement in water-wet porous media. In *Annual Review of Fluid Mechanics* (eds. M. van Dyke, J.V. Wehausen, and J.L. Lumley). Annual Reviews Inc., Palo Alto, CA. pp. 365-393.
- Pirkle W.A., Iversen G.M., and Tuck D.M. (1997a) DNAPL penetration of capillary barriers due to time-dependent wetting relationships. Final Report submitted in completion of SCUREF Project SC-00058, SCUREF Task 232. University of South Carolina-Aiken.
- Pirkle W.A., Iversen G.M., and Tuck D.M. (1997b) The effect of an organic dye on DNAPL entry pressure into water saturated porous media. Final report submitted in completion of SCUREF Project SC-0001-EC, SCUREF Task 185, Phase II. University of South Carolina-Aiken.
- Poulsen M.M. and Keuper B.H. (1992) A field experiment to study the behavior of tetrachloroethylene in unsaturated porous media. *Environ. Sci. Technol.* **26**, 889-895.
- Powers S.E. and Tamblin M.E. (1995) Wettability of porous media after exposure to synthetic gasolines. *J. Contam. Hydrol.* **19**, 105-125.
- Rayleigh L. (1879) On the capillary phenomena of jets. *Proc. Royal Soc. (London) A* **29**, 71-97.
- Rayleigh L. (1890) On the tension of recently formed liquid surfaces. *Proc. Roy. Soc. (London)* **47**, 281.
- Rideal E.K. and Sutherland K.L. (1952) The variation of the surface tension of solutions with time. Solutions of alcohols. *Trans. Farad. Soc.* **48**, 1109-1123.
- Rohlf F.J. and Sokal R.R. (1969) *Statistical Tables*. W. H. Freeman and Company, San Francisco.
- Schroth M.H., Istok J.D., Ahearn S.J., and Selker J.S. (1995) Geometry and position of light nonaqueous-phase liquid lenses in water-wetted porous media. *J. Contam. Hydrol.* **19**, 269-287.
- Scriven L.E. (1960) Dynamics of a fluid interface: Equation of motion for Newtonian surface fluids. *Chem. Eng. Sci.* **12**, 98-108.
- Slattery J.C. (1964) Surfaces-I. Momentum and moment of momentum balances for moving surfaces. *Chem. Eng. Sci.* **19**, 379-385.
- Slattery J.C. (1974) Interfacial effects in the entrapment and displacement of residual oil. *A.I.Ch.E. J.* **20**, 1145-1154.
- Slattery J.C. (1979) Interfacial effects in the displacement of residual oil by foam. *A.I.Ch.E. J.* **25**, 283-289.
- Sokal R.R. and Rohlf F.J. (1969) *Biometry: The Principles and Practice of Statistics in Biological Research*. W. H. Freeman and Company, San Francisco.
- Tartar H.V., Sivertz V., and Reitmeier R.E. (1940) The surface tension of aqueous solutions of some paraffin chain colloidal electrolytes, including a comparison of the capillary rise and sessile bubble methods of measurement. *J. Am. Chem. Soc.* **62**, 2375-2380.
- Tate T. (1864) On the magnitude of a drop of liquid formed under different circumstances. *Philos. Mag.* **27**, 176-180.
- Thomas W.D.E. and Potter L. (1975) Solution/air interfaces. I. An oscillating jet relative method for determining dynamic surface tensions. *J. Colloid Interface Sci.* **50**, 397-412.
- Tuck D.M. (1999) Discussion of "DNAPL migration through a fractured perching layer" by Daniel B. Stephens, James A. Kelsey, Mark A. Prieksat, Mel G. Piepho, Chao Shan, and Mark D. Ankeny. *Ground Water* **37**, 485-486.
- Tuck D.M. and Rulison C. (1999a) Azo dyes and their interfacial activity: Implications for multiphase flow experiments^(U). Westinghouse Savannah River Company, WSRC-MS-99-00138. Aiken, SC.
- Tuck D.M. and Rulison C. (1999b) Interfacial activity of Sudan IV dye in the tetrachloroethylene-water-glass system. Westinghouse Savannah River Company, WSRC-TR-98-0038. Aiken, SC.
- Tuck D.M., Iversen G.M., Pirkle W.A., and Rulison C. (1998) Time-dependent interfacial property effects on DNAPL flow and distribution. In *Nonaqueous-Phase Liquids: Remediation of Chlorinated and Recalcitrant Compounds* (eds. G.B. Wickramanayake and R.E. Hinchee). Battelle Press, Columbus, OH. pp. 73-78.
- Tuck D.M., Iversen G.M., and Pirkle W.A. (2000) DNAPL penetration of saturated porous media under conditions of time-dependent surface chemistry. In *Savannah River Site Environmental Remediation Systems in Unconsolidated Upper Coastal Plain Sediments - Stratigraphic and Structural Considerations: Carolina Geological Society 2000 Field Trip Guidebook, Aiken, SC* (eds. D.E. Wyatt and M.K. Harris). Carolina Geological Society. pp. K1-K16.
- Ward A.F.H. and Tordai L. (1944) Existence of time-dependence for interfacial tension of solutions. *Nature* **154**, 146-147.
- Ward A.F.H. and Tordai L. (1946) Time-dependence of boundary tensions of solutions. I. The role of diffusion in time-effects. *J. Chem. Phys.* **14**, 453-461.
- Zhang L.-H. and Zhao G.-X. (1989) Dynamic surface tension of the aqueous solutions of cationic-anionic surfactant mixtures. *J. Colloid Interface Sci.* **127**, 353-361.

